2594–2600 *Nucleic Acids Research, 2001, Vol. 29, No. 12*

Mutations in the TAR hairpin affect the equilibrium between alternative conformations of the HIV-1 leader RNA

Hendrik Huthoff and Ben Berkhout*

Department of Human Retrovirology, Academic Medical Center, University of Amsterdam, Meibergdreef 15, 1105 AZ Amsterdam, The Netherlands

Received February 8, 2001; Revised March 19, 2001; Accepted April 25, 2001

ABSTRACT

The HIV-1 untranslated leader RNA can adopt two mutually exclusive conformations that represent alternative secondary structures. This leader RNA can fold either an extended duplex through long-distance base pairing or a branched conformation in which the RNA locally folds into hairpin structures. Both leader RNA conformations have the TAR hairpin in common, which forms the extreme 5′ end of all HIV-1 transcripts. We report that truncation of the TAR hairpin shifts the equilibrium between the two RNA conformations away from the thermodynamically favored long-distance interaction. However, the equilibrium is partially restored in response to the cations Na^+ and Mg^{2+}. The transcripts with mutant TAR structures allowed us to investigate conditions affecting the competition between the alternative conformations of the HIV-1 leader RNA. We also demonstrate that the change in conformation of the leader RNA due to TAR truncations severely affects formation of the HIV-1 RNA dimer.

INTRODUCTION

The untranslated leader of the HIV-1 genome encodes several regulatory RNA motifs involved in both early replication steps (transcription, splicing and translation), as well as late replication functions (RNA dimerization, packaging and reverse transcription) (1). A well-known example of such a regulatory RNA motif is the TAR hairpin. This hairpin structure is located at the extreme 5′ end of HIV-1 transcripts and represents one of the best-documented regulatory viral RNA motifs. The structure of TAR is supported by biochemical studies, crystallography, phylogenetic analyses and viral evolution experiments (2–7). The role of TAR in Tat-mediated *trans*-activation of the HIV-1 LTR promoter is well established (8–11). Mutation of TAR has also been suggested to cause additional defects at other stages of the viral replication cycle, such as packaging of the viral RNA into virions and reverse transcription (12–17).

Recently, we have reported that the HIV-1 leader RNA can adopt alternating conformations and could potentially act as a molecular switch during the viral replication cycle (18). A novel conformation of the HIV-1 leader RNA was first identified as an unusually fast-migrating band on non-denaturing gels (19). Formation of this fast-migrating conformer was subsequently shown to depend on a long-distance interaction (LDI) between sequences of the poly(A) and dimer initiation signal (DIS) domains, which are located downstream of TAR in the HIV-1 leader RNA (Fig. 1A). The LDI base pairing is incompatible with the folding of local hairpin structures of the poly(A) and DIS domains, which are present in the alternative branched structure containing multiple hairpins (BMH, Fig. 1B). The LDI duplex is an extension of the stem formed by the primer binding site (PBS) domain (Fig. 1C), and represents the thermodynamically favored conformation of the HIV-1 leader RNA. This is supported by experimental evidence and computer-assisted structure prediction (18,19).

HIV-1 RNA dimerization proceeds through a kissing-loop mechanism by base pairing of the loop-exposed GCGCGC palindromes of two identical DIS hairpins (20–23). An important feature of the LDI conformation is the trapping of the DIS sequences, such that the dimerization signal is not exposed (Fig. 1C). We demonstrated that formation of the LDI indeed blocks dimerization, and mutants that prefer the BMH conformation readily dimerize (18). In order to form the RNA dimer, the wild-type HIV-1 leader RNA must undergo the LDI to BMH structural rearrangement to expose the DIS hairpin (Fig. 1B). This structural rearrangement is facilitated by the Gag-derived nucleocapsid (NC) protein, which possesses nucleic acid chaperone activity (18).

Although the 5′ TAR hairpin takes no direct part in LDI base pairing, transcripts with mutant TAR structures form this conformation with reduced efficiency (18). In this study, we investigated the influence of the HIV-1 TAR structure on the LDI:BMH equilibrium. We show that reduced LDI folding due to mutations in TAR does result in increased RNA dimerization, which is in accordance with a preference for the BMH conformation. However, the LDI folding defect of transcripts with mutant TAR structures can be overcome by adjustment of the buffer composition and the renaturation procedure. In particular, the cations Na^+ and Mg^{2+} influence the equilibrium between the LDI and BMH conformations of the HIV-1 leader RNA.

*To whom correspondence should be addressed. Tel: +31 20 566 4822; Fax: +31 20 691 6531; Email: b.berkhout@amc.uva.nl

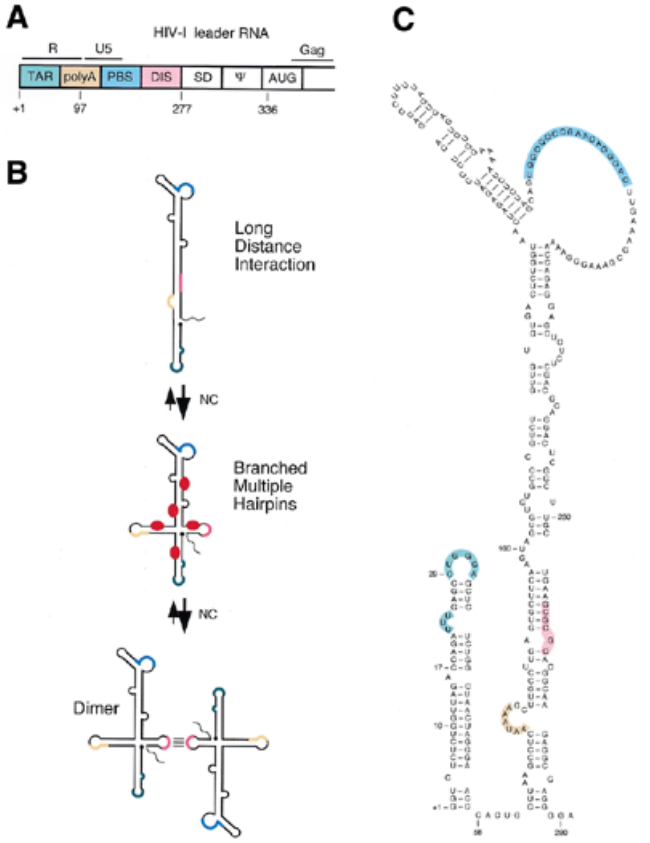

Figure 1. Structure and organization of the HIV-1 leader RNA. (**A**) Linear representation of the HIV-1 leader. Regions corresponding to previously proposed secondary structures are boxed and identified by abbreviations: the TAR hairpin, the poly(A) hairpin containing the AAUAAA hexamer, the U5-leader stem containing the PBS, the DIS, the splice donor site (SD), the major packaging signal (ψ) and the Gag start region (AUG). The positions of the R and U5 regions and the Gag open reading frame are indicated by lines. (**B**) Alternative secondary structures of the HIV-1 leader RNA. Several structure and sequence elements are highlighted: the TAR bulge and loop (green), the AAUAAA polyadenylation signal (orange), the PBS (blue) and the DIS palindrome (pink). The ground state conformation contains an extended R-U5-leader stem, which is the result of a LDI between the poly(A) and DIS domains. The alternate conformation exposes the poly(A) and DIS hairpins and takes the form of a BMH. The BMH monomer allows the formation of RNA dimers through base pairing of the palindromes of two DIS loops. The structural rearrangement from LDI to BMH is facilitated by the NC protein, which is indicated by red ovals on the BMH structure. (**C**) Detailed secondary structure model of the LDI conformation, color markings as in (B). Start sites of truncated transcripts are indicated at positions 10, 17, 29 and 58. The structure of the PBS region is according to (37) and Beerens,N., Groot,F. and Berkhout,B. (submitted for publication).

MATERIALS AND METHODS

In vitro transcription

RNAs were *in vitro* transcribed from PCR generated templates containing a T7 promoter directly upstream of the natural HIV-1 LAI +1 transcriptional start site or the indicated start positions. PCR was performed on the pBluescript 5′ LTR plasmid. The T7 promoter sequence was present in the sense primers, thus introducing the T7 promoter at desired positions. PCR fragments were precipitated with ethanol and washed before use in transcription reactions. Transcription was carried out with the Ambion megashortscript T7 transcription kit according to the manufacturer's instructions. Radiolabeled transcripts were synthesized in the presence of [α-^{32}P]UTP. Transcripts were subsequently excised from a 4% denaturing polyacrylamide gel (visualized by UV-shadowing or autoradiography) and eluted from the gel fragment by overnight incubation in 0.3 M Na acetate buffer (pH 5.2) at room temperature. The RNA was then precipitated and dissolved in water. Purified transcripts in water were heated to 85°C and allowed to slowly cool to room temperature. The stock solutions of RNA were stored at –20°C and aliquots were taken for subsequent analysis. Quantification of the RNA was done by UV-absorbance measurements and scintillation counting in case of radiolabeled transcripts.

In vitro RNA studies and non-denaturing electrophoresis

For electrophoretic analysis, ~10 ng of radiolabeled RNA was incubated in a final volume of 10 µl buffer. Buffers used: Tris (10 mM Tris–HCl pH 7.5), TEN buffer (100 mM NaCl, 10 mM Tris–HCl, EDTA pH 7.5) and TN buffer (100 mM NaCl, 10 mM Tris–HCl pH 7.5) supplemented with 0.1 or 1.0 mM $MgCl_2$. Initially, transcripts were incubated in TEN buffer at 37°C for 30 min (Fig. 2), but in subsequent experiments the RNA was heated to 60°C in the buffer and slowly cooled to room temperature. Annealing of antisense DNA was done in TEN buffer by heating to 60°C and subsequent cooling to room temperature. We used 100 ng of the antisense oligo CN1 (5′-GGTCTGAGGGATCTCTAGTTACCAGAGTC-3′), which is complementary to nucleotides 123–151 of the HIV-1 leader RNA and was selected from a set of antisense oligonucleotides that effectively denature the LDI conformer (19). Dimerization assays were carried out in a final volume of 10 µl dimerization buffer (40 mM NaCl, 0.1 mM $MgCl_2$ and 10 mM Tris–HCl pH 7.5). RNA concentration was varied as indicated for each sample (see Fig. 5). Dimerization samples were incubated at 60°C for 30 min and subsequently allowed to cool to room temperature.

After incubation, the samples were chilled on ice and diluted with 5 µl loading buffer (30% glycerol with BFB dye). Heat denaturation of control samples was carried out in formamide loading buffer by heating at 85°C. Samples were analyzed on a 4% polyacrylamide gel in 0.25 × TBE (22.5 mM Tris, 22.5 mM boric acid, 0.625 mM EDTA) or 0.25 × TBM (22.5 mM Tris, 22.5 mM boric acid, 0.1 mM $MgCl_2$). Native gels were run at 150 V at room temperature. Some samples were also analyzed on 6% sequencing gels containing urea.

RNA secondary structure prediction

Computer-assisted RNA secondary structure prediction was done using the Mfold v3.0 algorithm (24–26) offered by the MBCMR Mfold server (http://mfold.burnet.edu.au/). Settings were standard for all folding jobs, corresponding to conditions at 37°C and 1.0 M NaCl, using a 5% suboptimality range. The sequence of the HIV-1 B LAI isolate was downloaded from the HIV database (http://hiv-web.lanl.gov/). All truncated RNA species used in this study were analyzed by Mfold.

RNA absorbance melting curves

RNA thermal denaturation was monitored by measuring the absorbance of UV light at 260 nm in a quartz cuvette with a standard 1 cm path length. Absorbance was measured over a

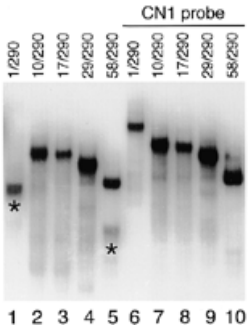

Figure 2. Non-denaturing gel electrophoresis of HIV-1 transcripts with increasing 5′ end truncations. 5′ and 3′ extremities of the transcripts are indicated at the top of the lanes, with numbering in relation to the transcriptional start site (+1). As a control, transcripts were annealed to the antisense oligo CN1 (lanes 6–10), which disrupt the LDI conformation of the HIV-1 leader RNA. Fast-migrating RNA species that adopt the LDI conformation are indicated by asterisks.

continuous temperature range from 10 to 95°C on a temperature controlled Perkin Elmer Lambda 2 spectrophotometer. Temperature was increased at a rate of 0.5°C/min with sampling at each 0.1°C. Samples contained ~3.0 µg of RNA dissolved in 140 µl of 50 mM Na cacodylate buffer (pH 7.2), supplemented with 0, 0.1 or 1.0 mM $MgCl_2$. Prior to the measurement, the RNA was renatured by incubation in the cacodylate buffer at 37°C for 30 min, after which $MgCl_2$ was added. Electrophoretic analysis of the samples prior to the analysis confirmed the monomeric state of the RNA (not shown). No significant degradation of the transcripts was apparent after the measurement, as judged by gel analysis (not shown).

RESULTS

Mutations in TAR affect the conformation of the HIV-1 leader RNA

As part of an extensive mutational analysis to identify the domains involved in formation of the LDI we analyzed HIV-1 transcripts with mutations in the 5′ TAR hairpin. A nested set of transcripts with variable 5′ ends was analyzed on a non-denaturing polyacrylamide gel (Fig. 2). This 5′ truncated set contains transcripts starting at nucleotide positions 10, 17, 29 and 58, as indicated in Figure 1C, and causes the stepwise disruption and eventual removal of the TAR hairpin. All transcripts share a common 3′ end, position 290, which extends beyond the minimal 3′ domain required for LDI formation (18). The wild-type 1/290 transcript forms the LDI and exhibits the characteristic fast electrophoretic mobility (Fig. 2, lane 1), which is lost after annealing of the antisense oligonucleotide CN1 (Fig. 2, lane 6). This antisense DNA binds to the U5 region of the HIV-1 leader RNA and effectively disrupts the LDI conformation (19). Transcripts starting at position 10, 17 and 29 produce a slow-migrating RNA (Fig. 2, lanes 2–4) that shows no significant change in mobility after annealing of the CN1 oligo (Fig. 2, lanes 7–9). Thus, it appears that these TAR-mutated transcripts are unable to form the LDI and instead adopt the BMH conformation. However, a faint band of fast mobility was observed for the 58/290 transcript lacking the complete TAR hairpin (Fig. 2, lane 5). This band is absent upon annealing of the CN1 oligo (Fig. 2, lane 10), and was not observed on denaturing gels (data not shown), suggesting that LDI formation is not completely dependent on the presence of the TAR hairpin.

HIV-1 transcripts with mutant TAR structures can be induced to adopt the LDI conformation

We tested a variety of renaturation protocols to assess LDI formation of transcripts with a mutant TAR structure. We found that slow rates of cooling during transcript renaturation significantly increased the fraction of transcripts that adopt the LDI (data not shown). The cationic constituents of the renaturation buffer also influence LDI formation. This is shown in Figure 3A, where transcripts 58/290, 17/290 and 1/290 were slowly cooled in a buffer lacking counterions and buffers containing 100 mM Na^+ with 0, 0.1 or 1.0 mM Mg^{2+}. The wild-type transcript adopts the LDI at ~70% efficiency in the buffer lacking counterions (Fig. 3A, lane 12). In the presence of Na^+, all of the wild-type transcripts form the LDI conformation (Fig. 3A, lane 13), and addition of Mg^{2+} has no further effect (Fig. 3A, lanes 14 and 15). Analysis of the mutant transcripts 58/290 and 17/290 yielded some interesting differences with the wild-type RNA. Both mutant transcripts do not form the LDI in the absence of counterions (Fig. 3A, lanes 2 and 7).

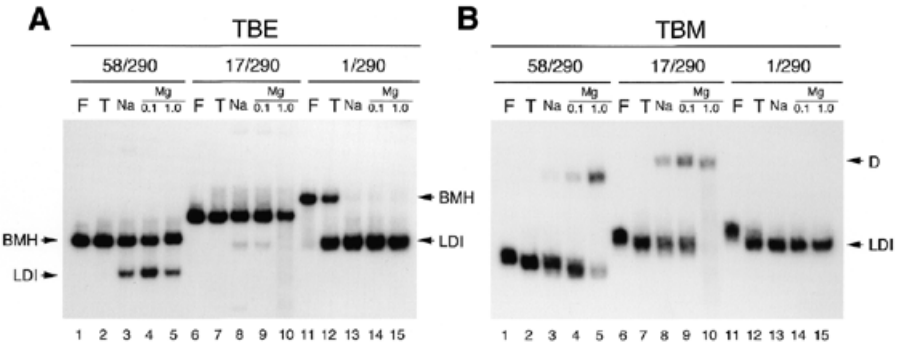

Figure 3. The effect of metal ions on the two conformations of the HIV-1 leader RNA. Transcripts were denatured in formamide (F), dissolved in Tris buffer (T) or renatured in the presence 100 mM Na^+ (lanes 3, 8 and 13) with increasing amounts of Mg^{2+} (0.1 mM, lanes 4, 9 and 14; 1.0 mM, lanes 5, 10 and 15). Samples were split and analyzed on a TBE gel (**A**) and TBM gel (**B**). The LDI, BMH and dimeric (D) conformations of the RNA are indicated by arrows.

Upon addition of Na^+, increased LDI formation is apparent for both transcripts (Fig. 3A, lanes 3 and 8). This effect is most prominent for the 58/290 transcript, which produces ~25% LDI in the presence of Na^+. The LDI fraction of this transcript is further increased to ~45% by the addition of 0.1 mM Mg^{2+} (Fig. 3A, lane 4). For transcript 17/290, no further stimulation of LDI folding is observed upon addition of 0.1 mM Mg^{2+} (Fig. 3A, lane 9). Intriguingly, raising of the Mg^{2+} concentration to 1.0 mM results in a reduction of the LDI fraction for both mutant transcripts (Fig. 3A, lanes 5 and 10). We thus observe that both stimulation and inhibition of LDI formation occurs in a Mg^{2+}-dependent manner.

To further investigate this effect, we analyzed the same samples on a non-denaturing gel containing 0.1 mM Mg^{2+} (TBM gel, Fig. 3B). Gels containing magnesium are commonly used in the study of HIV-1 RNA dimerization, as the kissing-loop RNA dimer does not resist electrophoresis in EDTA (21,27,28). On the TBM gel, the mutant transcripts produce both monomeric and dimeric RNA. In contrast with the results on the TBE gel (Fig. 3A), monomers of the mutant transcripts migrate as a single band on the TBM gel. The electrophoretic mobility of these monomers precisely follows the pattern of the LDI bands on the TBE gel. In particular, the 17/290 monomers have the same mobility as the wild-type 1/290 transcripts on the TBM gel. This suggests that the monomers observed on the TBM gel represent transcripts in the LDI conformation. This preference for the LDI structure on the TMB gel is reminiscent of the stimulatory effect of 0.1 mM Mg^{2+} on LDI formation observed on the TBE gel (Fig. 3A).

RNA dimers are observed on the TBM gel, but only for the TAR-mutated transcripts that preferentially adopt the BMH conformation on the TBE gel. As Mg^{2+} stimulates dimerization of HIV-1 RNA (20,28,29), this may explain the observed reduction in the LDI fraction of transcripts 58/290 and 17/290 at 1.0 mM Mg^{2+} on the TBE gel (Fig. 3A). Indeed, dimerization of the mutant transcripts 17/290 and 58/290 is nearly complete at 1.0 mM Mg^{2+} (Fig. 3B, lanes 5 and 10). Thus, the reduction in LDI formation observed on TBE gels at 1.0 mM Mg^{2+} (Fig. 3A) coincides with increased dimerization of these transcripts (Fig. 3B). The kissing-loop dimers formed in the presence of Mg^{2+} do not resist electrophoresis on the TBE gel, and apparently dissociate into BMH monomers, leading to the observed reduction of the LDI conformers.

Analysis of the transcripts on the TBM gel demonstrates a marked difference in dimerization efficiency of the wild-type and mutant transcripts (Fig. 3B). Dimers are apparent for the mutant transcripts 17/290 and 58/290, but not for the wild-type 1/290 transcript. Transcript 17/290 forms dimers up to nearly 100% efficiency in 1.0 mM Mg^{2+} (Fig. 3B, lane 10), and a low amount of dimers is formed without Mg^{2+} (Fig. 3B, lane 8). Dimerization is less efficient for transcript 58/290, reaching a maximum of 80% dimers at 1.0 mM Mg^{2+}. This mutant displays a more stringent Mg^{2+} requirement for dimerization at all conditions tested. In general, an inverse correlation between LDI formation and RNA dimerization is apparent. Efficient LDI formation follows the order 1/290 > 58/290 > 17/290 (Fig. 3A, TBE gel), and efficient dimer formation is observed in the order 17/290 > 58/290 > 1/290 (Fig. 3B, TBM gel). These results indicate that the LDI and RNA dimers represent mutually exclusive structures, which is consistent with the proposed base pairing schemes (Fig 1B).

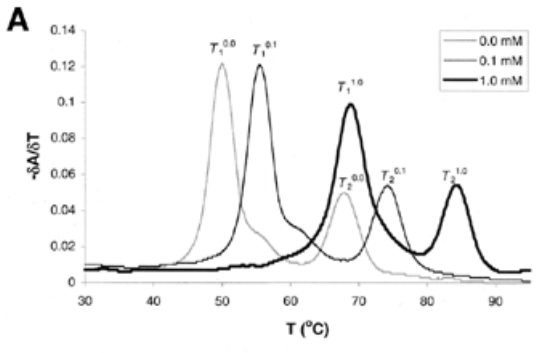

B

Mg^{++} (mM)	T_1 (°C)	$-\delta A/\delta T_1$	T_2 (°C)	$-\delta A/\delta T_2$
0.0	49.9	0.122	67.8	0.050
0.1	55.4	0.121	74.2	0.054
1.0	68.8	0.099	84.2	0.054

Figure 4. Thermal denaturation of the HIV-1 1/290 transcript at increasing Mg^{2+} concentrations, as monitored by UV absorption (λ = 260 nm). Curves for the first order derivative ($\delta A/\delta T$) are shown to allow for the accurate identification of melting transitions, T_1 and T_2. (**A**) Melting curves were obtained in the presence of 50 mM Na cacodylate (pH 7.5) with 0, 0.1 and 1.0 mM $MgCl_2$. (**B**) Values of T_1 and T_2 at increasing Mg^{2+} concentration, with corresponding $-\delta A/\delta T$ values at peak maximum.

The results described above support the notion that the BMH structure is the conformation of the monomeric RNA that allows formation of the RNA dimer. In particular, TAR mutants favor the BMH over the LDI structure, and therefore display a marked increase in RNA dimerization. We found that Mg^{2+} can stimulate both LDI and dimer formation of transcripts containing mutant TAR structures. Wild-type transcripts form the LDI conformation at all conditions tested, which explains the apparent inability of this RNA to dimerize readily. In summary, two important results derive from the experiments described above: (i) mutations in TAR lead to a preference for the BMH over the LDI structure (Fig. 3A, TBE gels), and thus favor RNA dimerization (Fig. 3B, TBM gels) and, (ii) the LDI:BMH equilibrium can be modulated by cations.

The effect of magnesium on the stability of the LDI conformation

Whereas wild-type HIV-1 transcripts do not require Mg^{2+} for LDI folding, the results with the TAR mutated transcripts suggest that Mg^{2+} increases the stability of this RNA conformation. To test this, we performed UV-absorbance melting experiments with the wild-type transcript in the absence and presence of Mg^{2+} (Fig. 4). The melting profile of the wild-type 1/290 transcript (Fig. 4A) is characterized by two major transitions in the absence of Mg^{2+}: a high intensity transition with T_m = 50°C (T_1) and a second transition of lower intensity at T_m = 67°C (T_2). We previously demonstrated that these transitions correspond to the LDI and the TAR hairpin, respectively (18).

Addition of increasing amounts of Mg^{2+} gradually shifts both peaks to higher temperatures (Fig. 4), demonstrating that Mg^{2+} stabilizes both the extended LDI duplex and the TAR hairpin. We did observe some broadening of transition T_1 at 1.0 mM Mg^{2+}, which is the result of melting over a wider temperature range. Broadening of this transition coincides with a decrease

in peak intensity, which is reflected in a decrease of the numerical value of δA/δT (Fig. 4B). This effect is not observed for transition T_2, suggesting that specific broadening of the LDI-associated melting transition T_1 at 1.0 mM Mg^{2+} is due to increased flexibility of this RNA domain. Thus, even though the LDI duplex may be stabilized by Mg^{2+}, the energy barrier between alternate conformations could be reduced. These results are consistent with the observation that both LDI formation and RNA dimerization benefit from Mg^{2+} (Fig. 3).

The LDI conformation of HIV-1 transcripts restricts RNA dimerization

The structure of monomeric HIV-1 leader transcripts is best described by an equilibrium between two alternate conformational states, the LDI and BMH structures (Fig. 1B). For wild-type transcripts, the LDI conformation is strongly favored. Mutations in TAR result in a shift towards the BMH structure, an effect that varies with the buffer composition (Fig. 3). This equilibrium between two alternate HIV-1 leader RNA conformations is further complicated by the observation that the BMH conformation allows subsequent formation of the RNA dimer. To further dissect this complex three state equilibrium of HIV-1 RNA structures, we performed dimerization assays at varying RNA concentrations, the reasoning being that RNA dimerization is sensitive to the RNA concentration because it represents an intermolecular base pairing interaction. We choose to compare the wild-type 1/290 transcript with the mutant 17/290 transcript, which has the most severe impact on the LDI:BMH equilibrium.

An increasing amount of unlabeled RNA was added to a 5 nM solution of radiolabeled RNA. Samples were allowed to dimerize and analyzed on a TBM gel (Fig. 5A). Bands were quantitated to determine the dimerization efficiency (Fig. 5B). As expected, both transcripts showed an increased dimerization efficiency in response to an increasing RNA concentration. However, the wild-type 1/290 transcript forms dimers much less efficiently than transcript 17/290, consistent with the results in Figure 3. At the lowest RNA concentration tested (5 nM), the wild-type 1/290 transcript forms monomers exclusively, whereas transcript 17/290 produces 16% dimers. At 50 nM RNA, dimerization yields remain <2% for the wild-type transcript, whereas the 17/290 transcript exceeds 50% dimers. Finally, transcript 17/290 yields almost exclusively dimers at RNA concentrations >250 nM, but the wild-type transcript yields at most 40% dimers at 2.0 μM.

The wild-type 1/290 transcript demonstrates reduced dimerization compared with the mutant 17/290 transcript at all RNA concentrations tested. Because the DIS sequence is identical in both transcripts, this result suggests that the differential dimerization capacities relate to the difference in conformation of these transcripts. The wild-type 1/290 preferentially adopts the LDI conformation and dimerization of this transcript necessitates the rearrangement into the BMH to expose the DIS hairpin. Thus, dimerization of the wild-type transcript follows a two-step mechanism: (i) an intramolecular structural rearrangement and (ii) the subsequent intermolecular interaction of two monomer BMH subunits. Transcript 17/290 preferentially adopts the BMH and dimerization of this transcript therefore does not require the LDI to BMH structural rearrangement. For this transcript, dimerization is essentially a one-step mechanism of association of two BMH conformers through DIS loop-kissing.

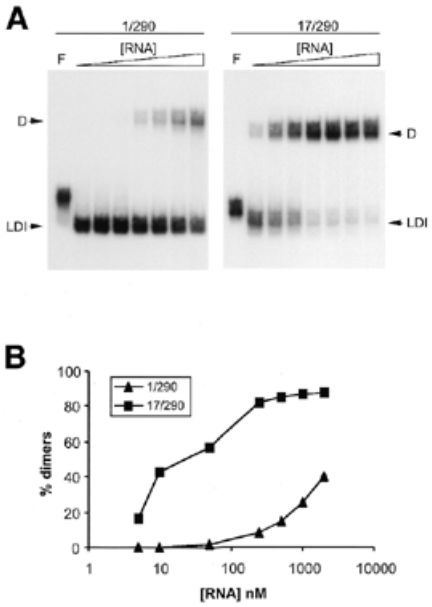

Figure 5. The effect of RNA concentration on formation of the HIV-1 RNA dimer. (**A**) Transcripts 1/290 and 17/290 were analyzed on a TBM gel. Increasing amounts of the corresponding unlabeled RNA were added to a solution of 5 nM radiolabeled transcripts. Final RNA concentrations: 5, 10, 50, 200 and 500 nM, 1 and 2 μM. Control samples were denatured in formamide as indicated by F. (**B**) Quantified data from the gel shown in (A).

DISCUSSION

We have studied the ability of wild-type and TAR-truncated HIV-1 leader transcripts to adopt two mutually exclusive conformations: the thermodynamically favored LDI between the poly(A) and DIS domains and the alternative BMH structure. Disruption of the TAR hairpin negatively influences formation of the LDI, thus resulting in a preference for the alternative BMH structure. In addition, we observed a strict inverse correlation between the effect of TAR mutations on LDI formation and RNA dimerization. Consistent with previous results with other HIV-1 RNA mutants that do not form the LDI (18), folding of the alternative BMH structure correlates with increased dimerization, which is known to proceed through the exposed DIS hairpin (20–22).

Deletion of TAR does not completely block LDI formation, and partial recovery of the LDI is achieved by adjusting buffer conditions. Specifically, LDI folding was significantly restored by addition of Na^+ and Mg^{2+} to the renaturation buffer, which is reminiscent of metal ion rescue of tertiary RNA structures (30,31). These results indicate that TAR is not essential for LDI formation, which is consistent with the proposed secondary structure model (Fig. 1). We observed that the defect in LDI formation is less severe for transcripts in which the complete TAR hairpin has been deleted than for transcripts with partial TAR deletions. The reduced LDI formation of the latter transcripts may be due to misfolding. Deletions in the 5′ side of the base paired TAR stem will render the 3′ complement single-stranded, and thus available for alternative base pairing. For instance, TAR nucleotides 51–57 share a high complementarity with nucleotides 105–111 just downstream of the poly(A) domain. Mfold analysis predicts this

base pairing scheme for transcripts containing truncated TAR structures (data not shown). Base pairing of nucleotides 51/57–105/111 extends the poly(A) hairpin by 5 additional Watson–Crick base pairs, and will therefore favor the BMH structure. We have previously demonstrated that stabilization of either the poly(A) or DIS hairpin inhibits formation of the LDI, and consequently results in increased dimerization (18). Removal of the complete TAR hairpin eliminates this misfolding possibility, thus explaining the intermediate phenotype of the 58/290 transcript. There is also some evidence that this misfolding trap is avoided *in vivo*. Evolution of HIV-1 viruses with a disrupted TAR stem through substitution of nucleotides 3–16 resulted in rapid acquisition of substitutions at positions 51–54, thereby eliminating base pairing to nucleotides 105–111 (7).

Deletion of the entire TAR hairpin does not completely relieve the preference for the BMH conformation, indicating that the structural integrity of TAR does affect the structure of the downstream leader RNA. The TAR hairpin and the LDI duplex are observed as independently structured domains in UV melting experiments. UV melting experiments suggest that the structural flexibility of the LDI, but not of TAR, is increased by Mg^{2+}. This was observed as peak-broadening of the LDI-associated melting transition at high Mg^{2+} levels. By increasing the number of conformational states accessible to this RNA domain, Mg^{2+} could reduce the energy barrier of the LDI to BMH structural rearrangement, and thus facilitate RNA dimerization. This idea is supported by the observation that the wild-type HIV-1 transcript produces reduced levels of LDI conformers at Mg^{2+} concentrations >5.0 mM (19). The effect of Mg^{2+} on the HIV-1 RNA conformation suggests that Mg^{2+} binds differentially to the LDI and BMH conformations, presumably through specific metal-coordination sites. Because Mg^{2+} concentrations may vary in different cellular compartments and in virion particles, this raises the interesting possibility that the HIV-1 leader RNA can adjust its structure in response to the chemical environment.

The melting transition associated with the TAR hairpin is not subject to broadening upon addition of magnesium, indicating that the TAR hairpin is a relatively rigid structure. In fact, this rigidity may be an important feature of the influence of TAR on the folding of the downstream leader domain. TAR could act as a scaffold for LDI-folding of the downstream RNA domain. This could be accomplished through co-axial stacking of adjacent helical domains or the stabilization of poly-helical junctions. Additional interactions may exist between TAR and the downstream HIV-1 leader RNA. For instance, the TAR loop is a potential candidate for additional base pairing interactions (32). However, in the course of these experiments we have not observed any evidence for such a tertiary interaction. In particular, the observation that the 58/290 transcript forms the LDI more efficiently than other TAR-mutated transcripts argues against the involvement of the TAR loop in a tertiary interaction. This was confirmed by electrophoretic and UV-melting analysis of transcripts in which the TAR loop sequence was mutated from CUGGGA to CUAAAA or UCAAAG, which did not affect LDI folding and RNA dimerization (data not shown).

A word of caution derives from the data presented in this study. We have demonstrated that 5′ TAR deletions have a considerable influence on the LDI:BMH equilibrium, and consequently on RNA dimerization. Studies on the dimerization of retroviral transcripts often make use of extensively truncated constructs. Our results demonstrate that the ability to perform the LDI to BMH structural transition is a key determinant in formation of the RNA dimer. The thermodynamically favored LDI conformation considerably inhibits the ability of HIV-1 RNA to dimerize. Taking into account this competition between two structural conformers of the HIV-1 leader RNA may help resolve the discrepancy between the results from *in vitro* and *in vivo* dimerization studies (12,33–36). Furthermore, the observation that mutations in HIV-1 TAR affect the conformation of the downstream leader RNA could account for some of the *in vivo* defects reported for TAR-mutated virus constructs. There is accumulating evidence that mutations in TAR affect virus replication mechanisms other than transcriptional activation. For instance, disruption of the TAR hairpin has been observed to affect RNA packaging and reverse transcription by several groups (12–17). We have previously postulated that the conformational polymorphism of the HIV-1 leader may act as a molecular switch in the viral replication cycle, thus accommodating regulatory signals for both the gene expression and genome packaging pathways (18). The data presented in this study demonstrate that mutations in the TAR hairpin significantly alter the RNA equilibrium that constitutes the regulatory switch. Thus, some of the virus replication defects observed upon mutation of TAR may be attributable to its influence on the structure of the downstream leader RNA.

ACKNOWLEDGEMENTS

We thank Jord Nagel and Cees Pleij for access to and assistance with the temperature-controlled spectrophotometer, Wim van Est for the artwork and Nancy Beerens for critical reading of the manuscript. This work was supported by the Netherlands Organization for Scientific Research (NWO-CW).

REFERENCES

1. Berkhout,B. (1996) Structure and function of the Human Immunodeficiency Virus leader RNA. *Progr. Nucleic Acids Res. Mol. Biol.*, **54**, 1–34.
2. Puglisi,J.D., Tan,R., Calnan,B.J., Frankel,A.D. and Williamson,J.R. (1992) Conformation of the TAR RNA–arginine complex by NMR spectroscopy. *Science*, **257**, 76–80.
3. Aboul-ela,F., Karn,J. and Varani,G. (1995) The structure of the human immunodeficiency virus type 1 TAR RNA reveals principles of RNA recognition by Tat protein. *J. Mol. Biol.*, **253**, 313–332.
4. Aboul-ela,F., Karn,J. and Varani,G. (1996) Structure of HIV-1 TAR RNA in the absence of ligands reveals a novel conformation of the trinucleotide bulge. *Nucleic Acids Res.*, **24**, 3974–3981.
5. Ippolito,J.A. and Steitz,T.A. (1998) A 1.3-Å resolution crystal structure of the HIV-1 *trans*-activation response region RNA stem reveals a metal ion-dependent bulge conformation. *Proc. Natl Acad. Sci. USA*, **95**, 9819–9824.
6. Berkhout,B. (1992) Structural features in TAR RNA of human and simian immunodeficiency viruses: a phylogenetic analysis. *Nucleic Acids Res.*, **20**, 27–31.
7. Klaver,B. and Berkhout,B. (1994) Evolution of a disrupted TAR RNA hairpin structure in the HIV-1 virus. *EMBO J.*, **13**, 2650–2659.
8. Muesing,M.A., Smith,D.H., Cabradilla,C.D., Benton,C.V., Lasky,L.A. and Capon,D.J. (1985) Nucleic acid structure and expression of the human AIDS/lymphadenopathy retrovirus. *Nature*, **313**, 450–458.
9. Fisher,A.G., Feinberg,M.B., Josephs,S.F., Harper,M.E., Marselle,L.M., Reyes,G., Gonda,M.A., Aldovini,A., Debouck,C. and Gallo,R.C. (1986) The *trans*-activator gene of HTLV-III is essential for virus replication. *Nature*, **320**, 367–371.

10. Berkhout,B., Silverman,R.H. and Jeang,K.T. (1989) Tat *trans*-activates the human immunodeficiency virus through a nascent RNA target. *Cell*, **59**, 273–282.
11. Wei,P., Garber,M.E., Fang,S.-M., Fisher,W.H. and Jones,K.A. (1998) A novel CDK9-associated C-type cyclin interacts directly with HIV-1 Tat and mediates its high-affinity, loop-specific binding to TAR RNA. *Cell*, **92**, 451–462.
12. Clever,J.L. and Parslow,T.G. (1997) Mutant human immunodeficiency virus type 1 genomes with defects in RNA dimerization or encapsidation. *J. Virol.*, **71**, 3407–3414.
13. Das,A.T., Klaver,B. and Berkhout,B. (1998) The 5′ and 3′ TAR elements of the human immunodeficiency virus exert effects at several points in the virus life cycle. *J. Virol.*, **72**, 9217–9223.
14. Clever,J.L., Eckstein,D.A. and Parslow,T.G. (1999) Genetic dissociation of the encapsidation and reverse transcription functions in the 5′R region of human immunodeficiency virus type 1. *J. Virol.*, **73**, 101–109.
15. Helga-Maria,C., Hammarskjold,M.L. and Rekosh,D. (1999) An intact TAR element and cytoplasmic localization are necessary for efficient packaging of human immunodeficiency virus type 1 genomic RNA. *J. Virol.*, **73**, 4127–4135.
16. Harrich,D., Hooker,C.W. and Parry,E. (2000) The human immunodeficiency virus type 1 TAR RNA upper stem–loop plays distinct roles in reverse transcription and RNA packaging. *J. Virol.*, **74**, 5639–5646.
17. Berkhout,B. (2000) Multiple biological roles associated with the repeat (R) region of the HIV-1 RNA genome. *Adv. Pharmacol.*, **48**, 29–73.
18. Huthoff,H. and Berkhout,B. (2001) Two alternating structures of the HIV-1 leader RNA. *RNA*, **7**, 143–157.
19. Berkhout,B. and van Wamel,J.L.B. (2000) The leader of the HIV-1 RNA genome forms a compactly folded tertiary structure. *RNA*, **6**, 282–295.
20. Skripkin,E., Paillart,J.C., Marquet,R., Ehresmann,B. and Ehresmann,C. (1994) Identification of the primary site of the human immunodeficiency virus type 1 RNA dimerization *in vitro*. *Proc. Natl Acad. Sci. USA*, **91**, 4945–4949.
21. Laughrea,M. and Jette,L. (1994) A 19-nucleotide sequence upstream of the 5′ major splice donor is part of the dimerization domain of human immunodeficiency virus 1 genomic RNA. *Biochemistry*, **33**, 13464–13474.
22. Mujeeb,A., Clever,J.L., Billeci,T.M., James,T.L. and Parslow,T.G. (1998) Structure of the dimer initiation complex of HIV-1 genomic RNA. *Nat. Med.*, **5**, 432–436.
23. Lodmell,J.S., Ehresmann,C., Ehresmann,B. and Marquet,R. (2000) Convergence of natural and artificial evolution on an RNA loop–loop interaction: the HIV-1 dimerization initiation site. *RNA*, **6**, 1267–1276.
24. Zuker,M. (1989) On finding all suboptimal foldings of an RNA molecule. *Science*, **244**, 48–52.
25. Zuker,M. and Turner,D.H. (1999) In Barciszewski,J. and Clark,B.F.C. (eds), *RNA Biochemistry and Biotechnology*. Kluwer Academic Publishers, Dordrecht/Boston/London, pp. 11–43.
26. Mathews,D.H., Sabina,J., Zuker,M. and Turner,D.H. (1999) Expanded sequence dependence of thermodynamic parameters improves prediction of RNA secondary structure. *J. Mol. Biol.*, **288**, 911–940.
27. Laughrea,M. and Jette,L. (1996) HIV-1 genome dimerization: formation kinetics and thermal stability of dimeric HIV-1LAI RNAs are not improved by the 1–232 and 296–790 regions flanking the kissing-loop domain. *Biochemistry*, **35**, 9366–9374.
28. Takahashi,K.-I., Baba,S., Chattopadhyay,P., Koyanagi,Y., Yamamoto,N., Takaku,H. and Kawai,G. (2000) Structural requirement for the two-step dimerization of human immunodeficiency virus type 1 genome. *RNA*, **6**, 96–102.
29. Jossinet,F., Paillart,J.-C., Westhof,E., Hermann,T., Skripkin,E., Lodmell,J.S., Ehresmann,C., Ehresmann,B. and Marquet,R. (1999) Dimerization of HIV-1 genomic RNA of subtypes A and B: RNA loop structure and magnesium binding. *RNA*, **5**, 1222–1234.
30. Feig,L.F. and Uhlenbeck,O.C. (1999) In Gesteland,R.F., Cech,T.R. and Atkins,J.F. (eds), *The RNA World*. Cold Spring Harbor Laboratory Press, Cold Spring Harbor, New York, NY, pp. 287–319.
31. Shan,S.O. and Herschlag,D. (2000) An unconventional origin of metal-ion rescue and inhibition in the *Tetrahymena* group I ribozyme reaction. *RNA*, **6**, 796–813.
32. Chang,K. and Tinoco,I. (1997) The structure of an RNA 'kissing' hairpin complex of the HIV TAR hairpin loop and its complement. *J. Mol. Biol.*, **269**, 52–66.
33. Berkhout,B. and van Wamel,J.L.B. (1996) Role of the DIS hairpin in replication of human immunodeficiency virus type 1. *J. Virol.*, **70**, 6723–6732.
34. Haddrick,M., Lear,A.L., Cann,A.J. and Heaphy,S. (1996) Evidence that a kissing loop structure facilitates genomic RNA dimerisation in HIV-1. *J. Mol. Biol.*, **259**, 58–68.
35. Paillart,J.-C., Berthoux,L., Ottmann,M., Darlix,J.-L., Marquet,R., Ehresmann,B. and Ehresmann,C. (1996) A dual role of the putative RNA dimerization initiation site of human immunodeficiency virus type 1 in genomic RNA packaging and proviral DNA synthesis. *J. Virol.*, **70**, 8348–8354.
36. Laughrea,M., Shen,N., Jette,L. and Wainberg,M.A. (1999) Variant effects of non-native kissing-loop hairpin palindromes on HIV replication and HIV RNA dimerization: role of stem–loop B in HIV replication and HIV RNA dimerization. *Biochemistry*, **38**, 226–234.
37. Damgaard,C.K., Dyhr-Mikkelsen,H. and Kjems,J. (1998) Mapping the RNA binding sites for human immunodeficiency virus type-1 Gag and NC proteins within the complete HIV-1 and -2 untranslated leader regions. *Nucleic Acids Res.*, **26**, 3667–3676.